

# MACHINE LEARNING ANALYSIS OF COMPLEX NETWORKS IN HYPERSPHERICAL SPACE\*

MARÍA PEREDA<sup>†</sup> AND ERNESTO ESTRADA<sup>‡</sup>

**Abstract.** A complex network is a condensed representation of the relational topological framework of a complex system. A main reason for the existence of such networks is the transmission of items through the entities of these complex systems. Here, we consider a communicability function that accounts for the routes through which items flow on networks. Such a function induces a natural embedding of a network in a Euclidean high-dimensional sphere. We use one of the geometric parameters of this embedding, namely the angle between the position vectors of the nodes in the hyperspheres, to extract structural information from networks. Such information is extracted by using machine learning techniques, such as nonmetric multidimensional scaling and K-means clustering algorithms. The first allows us to reduce the dimensionality of the communicability hyperspheres to 3-dimensional ones that allow network visualization. The second permits to cluster the nodes of the networks based on their similarities in terms of their capacity to successfully deliver information through the network. After testing these approaches in benchmark networks and compare them with the most used clustering methods in networks we analyze two real-world examples. In the first, consisting of a citation network, we discover citation groups that reflect the level of mathematics used in their publications. In the second, we discover groups of genes that coparticipate in human diseases, reporting a few genes that coparticipate in cancer and other diseases. Both examples emphasize the potential of the current methodology for the discovery of new patterns in relational data.

**Key words.** networks, clustering algorithms, geometric embedding, communicability, matrix functions, network communities

**AMS subject classifications.** 68Q25, 68R10, 68U05

**1. Introduction.** Complex networks represent a vast category of data systems describing the topological organization of many complex systems, ranging from social, technological and ecological to molecular ones [43, 12, 37, 5]. The representation of this type of data as networks provides information about the topological, spatial, and functional relations of the data. In mathematical terms, networks are graphs—simple, directed and/or weighted—in which nodes represent the entities of the system and edges represent relations between such entities. The simplest of all the possible representations of networked data is by means of simple graphs. In this case only the connectivity between entities is captured by the graph, excluding other structural factors such as directionality, nature of nodes and strength of relations. Thus, an important challenge in this modeling scenario is to extract as much information as possible from this reduced representation of the data. Thus, the use of data analysis techniques, such as machine learning [51], is an important research area of analysis for networked type of data.

Machine learning stands at developing computational methods for “learning” with accumulated experiences, either in a supervised or an unsupervised way [32, 10, 59]. In supervised learning the inference of concepts from the data is performed from a training set [2]. Then, the learning process constructs a mapping function from this training, which can then be applied to data not “seen” before by the model.

---

\*Submitted to the editors DATE.

<sup>†</sup>RWTH Aachen University, Chair for Computational Social Sciences and Humanities, Germany. Grupo Interdisciplinar de Sistemas Complejos, Departamento de Matemáticas, Universidad Carlos III de Madrid. Unidad Mixta Interdisciplinar de Comportamiento y Complejidad Social (UMICCS), Spain. [maria.pereda@humtec.rwth-aachen.de](mailto:maria.pereda@humtec.rwth-aachen.de)

<sup>‡</sup>Department of Mathematics and Statistics, University of Strathclyde, 26 Richmond Street, Glasgow, UK. [ernesto.estrada@strath.ac.uk](mailto:ernesto.estrada@strath.ac.uk)

These models correspond either to those of classification or regression. On the other hand, the main goal of unsupervised learning is to reveal intrinsic structures that are embedded within the data relationships [25]. In this case, the algorithms are designed to learn solely guided by the structure of the data provided without any prior knowledge about the data. The typical unsupervised learning techniques are: clustering [33, 30, 29, 34], outlier detection [38, 40], dimensionality reduction [55], and association [47].

An area of unsupervised machine learning on networked systems which has received a great deal of attention is graph/network clustering [50, 48, 19, 21, 22]. In general, the problem consists on the unsupervised detection of groups of nodes—known as communities in network theory [48, 19, 21, 22]—which share more similarity among them than with nodes outside these clusters. The main interest in network clustering is due to its numerous applications, making the problem of graph clustering a data-driven task. The most frequently used definition of community in networks is the one based on edge density. For instance, in her 2007 overview of graph clustering Schaeffer [50] recall that *“it is generally agreed upon that a subset of vertices forms a good cluster if the induced subgraph is dense, but there are relatively few connections from the included vertices to vertices in the rest of the graph”*. In his seminal overview of 2010 Fortunato [19] pointed out that *“communities in graphs are related, explicitly or implicitly, to the concept of edge density (inside versus outside the community)”*. He makes clear the difference with data clustering where *“communities are sets of points which are “close” to each other, with respect to a measure of distance or similarity, defined for each pair of points”*. More recently, Silva and Zhao [51] in their book tacitly define a community: *“as a subgraph whose vertices are densely connected within itself, but sparsely connected with the remainder of the network”*. However, the complexity of graphs representing real-world systems is sufficiently large for not having to restrict our definition of clusters to those based on edge density only. As a data-driven problem our main task is to design methods that allow the detection of clusters of nodes/edges which are structurally similar to each other and that may contain important functional information about the processes taking place on real-world systems.

Let us consider here an example for motivating the use of other definitions of clustering on graphs/networks. Suppose that there is strong empirical evidence that groups of fused triangles—which can be formally defined in mathematical terms—represent functional groups for certain classes of real-world networks. In Fig.1 we illustrate a hypothetical network displaying three clusters of fused triangles represented in three different colors. Even by eye we can see that there are two “communities” according to the traditional definition based on edge density. Thus, this means that every method designed to detect density-communities will fail in detecting the fused-triangle clusters in this network. It does not mean that a method designed to detect such triangle-based structures is better or worse than the ones to detect density-communities. They simply are designed for performing different tasks on the same dataset.

With the goal of enriching the structural information contained in graph clustering a series of methods have been proposed which use the embedding of the graphs in geometric spaces. For instance, Xiao and Hancock [57] embed graphs using the heat-kernel and then by equating the spectral heat kernel and its Gaussian form they are able to approximate the Euclidean distance between nodes on the manifold. After this they perform principal component analysis (PCA) and demonstrate that it leads to well defined graph clusters. Other approaches use tools from subspace analysis on a Grassmann manifold to produce low dimensional representation of the original graphs

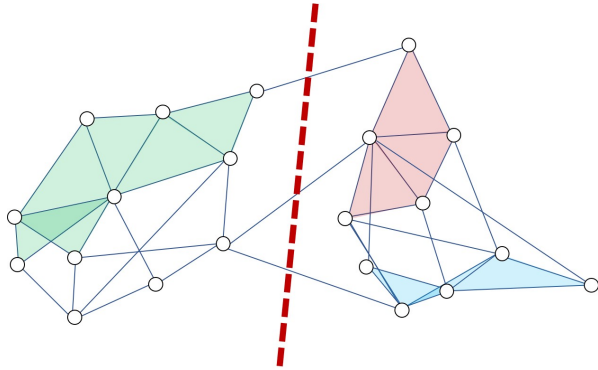


Fig. 1: Illustration of a hypothetical network in which three clusters based on fused-triangles exist. Any community detection method based on cluster density will fail in identifying such clusters as they will report the existence of two dense communities connected by three edges only as indicated by the red broken line.

which preserves important structural information [11]. Others embed the networks into hyperbolic space such that network community structure is obtained from node similarity in such “*underlying hidden metric space*” [42]. In general, these methods can be grouped under the umbrella of “*geometric learning*” methods [7]. Many of these algorithms are based on spectral techniques on graphs [56, 45]. Specifically, these approaches propose to embed the vertices of the original graph into a low dimensional space, which consists of the top eigenvectors of a special matrix and then carrying out the clustering in such low dimensional spaces [7].

Here we propose a new approach that can be enclosed in the category of geometric unsupervised learning. However, instead of “imposing” an embedding of the network in a given manifold we consider the geometric space generated by the flow of “items” on a network in a diffusion-like process. This space is a Euclidean  $(n - 1)$ -sphere, where  $n$  is the number of nodes of the graph. Using this approach, without the necessity of dimensionality reduction, we are able to identify clusters in networks, which not necessarily depend only on their edge density. After testing the method in a few benchmark networks we embarked in the analysis of two real-world systems. One is a citation network and the other a network of gene co-participation in human genetic diseases. In the first case we discovered the existence of groups of authors which mainly represent wide-range of disciplines mainly demarked by their level of mathematization. In the second example we discover a few genes which co-participate in neurological diseases and cancer, as well as in other groups of diseases and cancer. Using nonmetric multidimensional scaling we make a dimensionality reduction of the hyperspheric spaces to 2-spheres, which allow a nice visualization of the communicability space of networks.

**2. Preliminaries .** Here we follow standard notation and definitions in network theory (see for instance [12]). Let  $\Gamma = (V, E)$  be a simple graph and let  $A$  be its adjacency matrix. We consider here undirected graphs such that the associated adjacency matrix is symmetric, and its eigenvalues are real. We label the eigenvalues of  $A$  in non-increasing order:  $\lambda_1 \geq \lambda_2 \geq \dots \geq \lambda_n$ . Since  $A$  is a real-valued, symmetric matrix, we can decompose  $A$  into  $A = U\Lambda U^T$ , where  $\Lambda$  is a diagonal matrix containing

the eigenvalues of  $A$  and  $U = [\vec{\psi}_1, \dots, \vec{\psi}_n]$  is orthogonal, where  $\vec{\psi}_i$  is an eigenvector associated with  $\lambda_i$ . Because the graphs considered here are connected,  $A$  is irreducible and from the Perron-Frobenius theorem we can deduce that  $\lambda_1 > \lambda_2$  and that the leading eigenvector  $\vec{\psi}_1$ , which will be sometimes referred to as the *Perron vector*, can be chosen such that its components  $\psi_1(u)$  are positive for all  $u \in V$ . A row of the matrix  $U$  corresponding to the node  $i$  of the graph is designated here by the vector  $\vec{\varphi}_i = [\psi_1(i), \dots, \psi_n(i)]^T$ .

An important quantity for studying communication processes in networks is the so-called communicability function [13, 16, 15]. Let  $u$  and  $v$  be two nodes of  $\Gamma$ . The communicability function between these two nodes is defined as

$$(2.1) \quad G_{uv} = \sum_{k=0}^{\infty} \frac{(A^k)_{uv}}{k!} = (\exp(A))_{uv} = \sum_{k=1}^n e^{\lambda_k} \psi_k(u) \psi_k(v).$$

It counts the total number of walks starting at node  $u$  and ending at node  $v$ , weighted in decreasing order of their length by a factor  $\frac{1}{k!}$ . That is, the communicability function considers shorter walks more influential than longer ones and penalize them appropriately such that the whole series converges. The  $G_{uu}$  terms of the communicability function characterize the degree of participation of a node in all subgraphs of the network, giving more weight to the smaller ones. Thus, it is known as the subgraph centrality of the corresponding node [17].

**3. Hyperspherical Embedding of Networks.** An important property of the communicability function of networks is that it induces an embedding of the network into a given Euclidean space. The important parameter in this case is the difference between the number of weighted closed walks that start at (and return to) the corresponding nodes  $u$  and  $v$ , and the number of weighted walks that start at node  $u$  (respectively  $v$ ) and ends at the node  $v$  (respectively  $u$ ). This difference, which is defined below as  $\xi_{uv}^2$  serves as a quantification of the potential quality of communication channels between two nodes. That is, if there are many routes that connect nodes  $u$  and  $v$  together, and there are not many routes that starting at the node  $u$  (respectively  $v$ ) return to it, we can say that most of “information” departing the node  $u$  (respectively  $v$ ) with destination to the node  $v$  (respectively  $u$ ) will arrive at it. Thus, there is a potential good quality of communication between these two nodes. The other way around is very clear as if there are many returning routes to the nodes and very few connecting them, most of the information departing one node will never arrive at the other. Let us now define these terms formally. Based in the previous intuition we define the following quantity:

$$(3.1) \quad \xi_{uv}^2 = G_{uu} + G_{vv} - 2G_{uv}$$

Because  $G = \exp(A)$  is positive definite we can express it as a Gram matrix of the form

$$(3.2) \quad G = X^T X,$$

where  $X = [\vec{x}_1, \dots, \vec{x}_n]$  and

$$(3.3) \quad \vec{x}_u = \exp(A/2) \vec{\varphi}_u,$$

It is straightforward to realize that

$$\begin{aligned}
\vec{x}_u \cdot \vec{x}_u &= (\exp(\Lambda/2) \vec{\varphi}_u)^T \exp(\Lambda/2) \vec{\varphi}_v \\
&= \vec{\varphi}_u^T \exp(\Lambda/2) \exp(\Lambda/2) \vec{\varphi}_v \\
(3.4) \quad &= \vec{\varphi}_u^T \exp(\Lambda) \vec{\varphi}_v \\
&= \sum_{k=1}^n e^{\lambda_k} \psi_k(u) \psi_k(v) \\
&= G_{uv}.
\end{aligned}$$

Then, we can express  $\xi_{uv}^2$  in terms of the vectors  $\vec{x}_u$  and  $\vec{x}_v$  as

$$\begin{aligned}
(3.5) \quad \xi_{uv}^2 &= \vec{x}_u \cdot \vec{x}_u + \vec{x}_v \cdot \vec{x}_v - 2\vec{x}_u \cdot \vec{x}_v \\
&= \|\vec{x}_u - \vec{x}_v\|^2,
\end{aligned}$$

which means that  $\xi_{uv}^2$  is a Euclidean distance (metric) between the corresponding nodes and that  $\vec{x}_u$  is the position vector of the corresponding node in such Euclidean space. Previously we have proved that such embedding space is an  $n$ -dimensional sphere [18]. That is, the communicability distance  $\xi_{uv}^2$  induces an embedding of the graph  $\Gamma$  of size  $n$  into an  $(n-1)$ -sphere, of radius  $R^2 = \frac{1}{4} \left( c - \frac{(2-b)^2}{a} \right)$ , where  $a = \vec{1}^T \exp(-A) \vec{1}$ ,  $b = \vec{s}^T \exp(-A) \vec{1}$ ,  $c = \vec{s}^T \exp(-A) \vec{s}$ , and  $\vec{s} = \text{diag}(\exp(A))$ . The angles between the position vectors of the nodes  $u$  and  $v$  in the  $(n-1)$ -sphere are then given by [14]

$$(3.6) \quad \theta_{uv} = \cos^{-1} \frac{G_{uv}}{\sqrt{G_{uu}G_{vv}}}.$$

A pictorial representation of the communicability-induced geometry of a graph is given in Figure 2 for the case of a path graph with three nodes  $P_3$ . In this case the embedding is realized in a 3-dimensional sphere (2-sphere). The communicability distance is the chord between the two corresponding nodes embedded in the sphere and the communicability angle is the one formed between the centre of coordinates and the two corresponding nodes.

The communicability angle is defined as the ratio between the weighted number of walks connecting the two nodes to the number of walks starting and ending at the same node. Thus, it also quantifies the goodness of communication channels between the two nodes. However, while the communicability distance is unbounded—it can take an infinite value for infinitely large graphs—the communicability angle is bounded as  $0^\circ \leq \theta_{uv} \leq 90^\circ$  [14], where the lower bound is reached for pairs of nodes communicating with exceptionally good quality and the upper bound is reached for pairs of nodes communicating in a very bad way. The communicability angle is then a way of quantifying how efficiently a network uses the communication space available to it. For instance, the average communicability angles for the connected graphs with four nodes are: Path ( $59.09^\circ$ ), Star ( $55.37^\circ$ ), Cycle ( $45.11^\circ$ ), triangle with a pendant node ( $44.97^\circ$ ), and complete graph ( $21.48^\circ$ ). Clearly, the path graph is the least efficient one, followed by the star—which are the only two trees in this set—, then the graph consisting of a triangle and a pendant node, the cycle and finally the complete graph. This order agrees very well with our intuition corresponding to the average communication efficiency of these graphs. For all the previous reasons hereafter we concentrate our study on the communicability angles instead of the communicability distances.

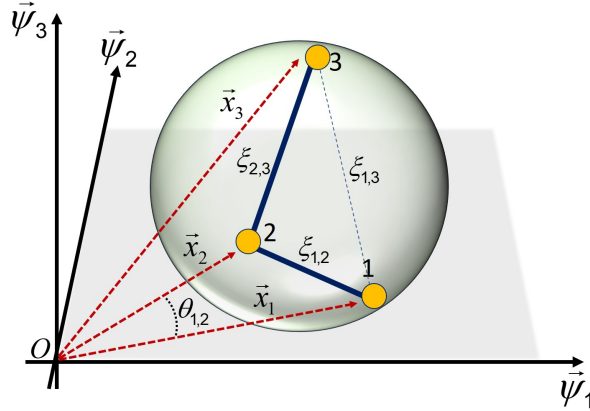


Fig. 2: Illustration of the embedding of a simple graph with 3 nodes into a 2-sphere. See main text for the description of the terms involved.

**4. Nonmetric Multidimensional Scaling and Visualization.** The hyperspherical embedding induced by the communicability geometry of a network does not allow to visualize the corresponding network due to the high dimensionality of the embedding spaces. Then, we aim here to reduce such space dimensionality to a 3-dimensional (3D) Euclidean space which allow us to visualize the network structure. We selected the 3D space as it represents the largest dimensionality that we can visualize with the minimum loss of information. There are several techniques that can be used for this dimensionality reduction [6]. Here we selected the nonmetric multidimensional scaling (NMDS) mainly due to the following reasons. In NMDS [36, 35] we select a priori the number of axis that we wish—3 in this case—instead of the many axis selected by most of ordination methods. Also NMDS is a numerical method that iteratively searches for a solution stopping when an acceptable solution (or a predetermined number of iterations). NMDS is not an eigen-method like PCA or correspondence analysis in which axis explain the variance of the data in a given order according to the magnitude of the corresponding eigenvalue. Finally, NMDS makes little assumptions about the data points which makes it very suitable for a wide variety of data. A clear disadvantage of NMDS with respect to other ordination methods is that its solution is not unique due to its numerical nature. However, the current availability of more powerful computational resources allows the execution of several realizations with different initial conditions, to select the best possible solution in a way that avoids getting trapped in local minima due to the use of an heuristic algorithm. In general, multidimensional scaling can be defined as a *method that represents measurements of similarity (or dissimilarity) among pairs of objects as distances among points of a low-dimensional multidimensional space*” [6].

Here we consider the matrix  $\theta = [\theta_{pq}]_{n \times n}$  as our similarity matrix. That is two nodes of a graph/network are similar if they have communicability angles close to  $0^\circ$  and dissimilar if they have an angle close to  $90^\circ$ . We then transform this matrix as described in the Supplementary Information to directly apply NMDS.

In order to avoid getting trapped into local minima, we make a series of replications, with different initial random configurations, and we select the ordination with the best fit. In addition of this nonmetric scaling for the dissimilarities we have

also implemented metric scaling ones. In particular we consider the following four metric scaling: 'metricstress', which calculates the stress, normalized with the sum of squares of the dissimilarities, 'metricsstress', which calculates the squared stress, normalized with the sum of 4th powers of the dissimilarities; 'sammon', which obtains Sammon's nonlinear mapping criterion, and 'strain', which is a criterion equivalent to that used in classical multidimensional scaling. All of these metrics are implemented in Matlab<sup>®</sup>.

As we have different metrics we will obtain different "best" reduced angle matrices, one for each of scaling used. We noticed that the root mean square error (RMSE) between the  $n$ -dimensional angle matrix and the reduced 3D one was fooled by those angles which were relatively close in both matrices although there were angles which differed significantly from each other in the two matrices (see further example). Instead of using RMSE as comparison method, we propose a spectral comparison between the two matrices. That is, we calculated the eigen-distance between  $\theta$  and  $\hat{\theta}$  (estimated angles in the 3D space) from their eigenvalues. In this way we compute the sum of the squares of the difference between the eigenvalues of both matrices as our measure of quality of the fit to compare the different methods. In Table ?? we give an example of the use of NMDS for reducing the dimensionality of the communicability angle matrix to a three-dimensional space.

We then consider some random networks based on three different construction methods. The first is based on the Erdős-Rényi (ER) model [46], the second is based on the Barabási-Albert (BA) model [3] and the two others are based on the  $\beta$ -skeleton method for generating spatial graphs [54, 31], in particular we study the Gabriel graph ( $\beta = 1$ ) [24] and the relative neighborhood graph ( $\beta = 2$ ) [54]. In all cases the networks constructed have 100 nodes and the number of edges depended on the type of method used, e.g. 200 for ER, 191 for BA and 118 for the spatial networks. In Figure3 we illustrate the 3D representation of these four networks after the reduction of the dimensionality of the communicability hyperspace using the multidimensional scaling method. The best scaling were produced by Sammon (ER, Gabriel and RNG) and by metricstress (BA) and the values of SE are: 347.97 (ER), 366.06 (BA), 348.02 (Gabriel) and 313.88 (RNG).

**5. Cluster Analysis.** In our context of network analysis the problem of clustering in the multidimensional communicability space consists in having nodes close to each other if they share certain structural similarities which make them to cluster together, while those structural dissimilar nodes are placed far apart in the 3D embedding studied here. The problem of clustering is one of the most popular tasks in machine learning and data science in general. Its main goal is to divide a set of objects into clusters in an unsupervised manner, such that those objects in a cluster are similar to each other and somehow dissimilar to those on other clusters. In the context of network analysis this problem is mainly studied for the detection of the so-called network communities. We point the reader to [48, 19, 21, 22] for overviews on the most used community detection techniques in networks. Most of these methods are defined on the basis of the internal density of links in the clusters and its relation to the inter-cluster density of links. Although this density-based definition is theoretically appealing it leaves a lot of other possibilities outside its scope (see introduction). In contrast, here we define a cluster as a homogeneous group of nodes in terms of their communicability angles in the multidimensional communicability hypersphere in which the network is embedded. We know that a characteristic feature of multidimensional scaling is that it produces an embedding of the data points



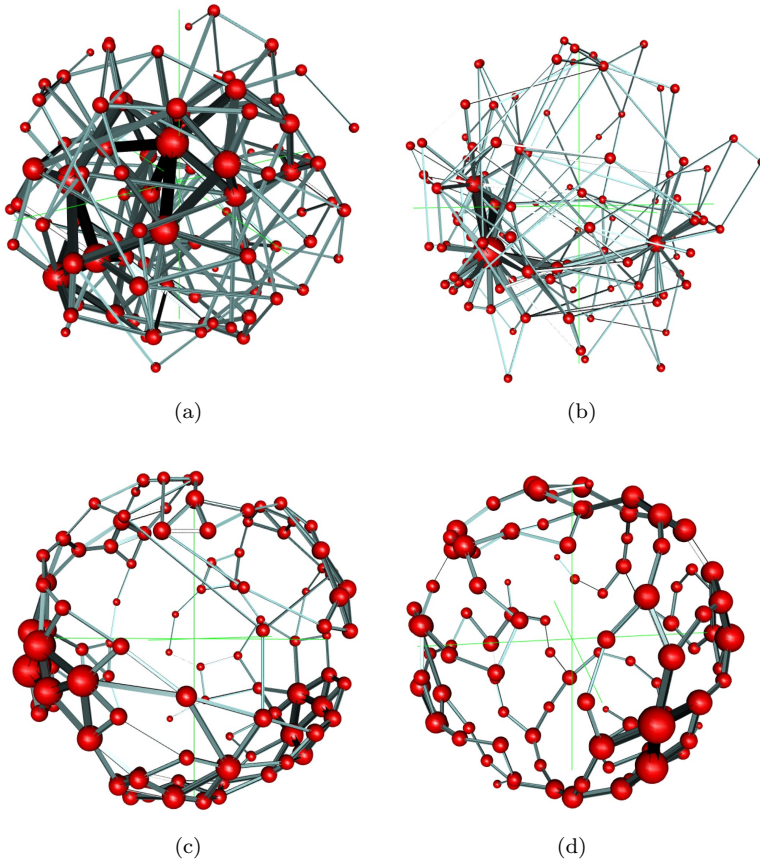


Fig. 3: Illustration of the plot of random graphs on the reduced 3D space of communicability angles obtained by nonmetric multidimensional scaling. (a) Erdős-Rényi (ER) graph with  $n = 100$ , and  $m = 200$ , (b) Barabási-Albert (BA) graph with  $n = 100$ , and  $m = 191$ , (c) spatial Gabriel graph with  $n = 100$ , and  $m = 118$  and (d) Relative Neighborhood Graph (RNG) with  $n = 100$ , and  $m = 118$ . The two spatial graphs in (c) and (d) are special cases of  $\beta$ -skeleton graphs with  $\beta = 1$  and  $\beta = 2$ , respectively.

into a reduced space such that the points which are located close to each other are similar according to some empirical characteristic, and those that are far apart are different. Thus, we also analyze the clustering problem of nodes in networks using the reduced 3D space produced by the multidimensional scaling studied in this work. In both cases, we expect that the nodes inside a cluster are homogeneous in terms of their total or “reduced” communicability angles, and nodes in different clusters are expected to be heterogeneous in this respect. These clusters may be or may be not related to density-based communities, but in any case we have a clear unambiguous definition of them.

In this work we aim at finding communicability clusters in the sense of K-Means [29, 52], i.e., we propose a partitional clustering method [19] using the embedding induced by the communicability function. Our selection of this method is based on its great popularity for detecting clusters in an unsupervised manner, which have



produced a large number of documented examples of applications in areas such as cheminformatics, bioinformatics, data mining, natural language processing, among others. We also know the main drawbacks of this method, mainly the fact that K-Means does not guarantee a convergence to a global minimum, with its final clusters heavily dependent on the initial centroids ??.

Due to the fact that we have to pre-select the number of clusters  $K$  we need to compare the quality of the partition for the different values of the number of clusters selected. With this goal we use several cluster validity indexes (CVIs) for estimating  $K$  [28, 39]. Here we use three popular CVIs, namely the Calinski-Harabasz index [8], the Silhouette index [49], and the Davies-Bouldin index [9], which are described in the Supplementary Information accompanying this paper.

**5.1. Resolution.** One of the most important problems that have been detected when studying clustering problems on networks is that of the so-called resolution limit [20]. The problem is simply described as the gluing of small clusters produced by some clustering methods—particularly those based on modularity—when there are many of such small highly connected clusters which are loosely connected among them. The paradigmatic example of the resolution limit is given by the caveman network illustrated in Fig.4 (a) in which every solid circle represents a clique. In this type of situation, modularity-based methods detect half the number of clusters existing in the network due to the merging of clusters by pairs as indicated in Fig.4 (a) by the broken red ellipses. We have tested the current method for the existence of such resolution limit problem and the results are illustrated in Fig.4 (b) and (c) for the use of the Silhouette method using the full-dimensional communicability angle matrix. The results are exactly the same for the reduced communicability angle matrix as well as for the three different CVIs used here. As can be seen the Silhouette index has a clear maximum peak at  $K = 10$  indicating the existence of the 10 expected communities, each of them formed by a clique of 5 nodes. In Fig.4 (c) we illustrate the plot of the communities in the reduced 3D space using the nonmetric multidimensional scaling method previously described. It is easy to see that each cluster is well separated from each other in the graphic and that the nodes in each clique are grouped together in a close space. The resolution problem is only one of the several situations that we can find when studying clustering of points. A group of these situations have been studied by Liu et al. [39] and they include, apart from the desired case of well-separated clusters, the existence of noisy clusters, subclusters, clusters distributed in a skew way and the presence of clusters of different densities (see Fig.5 for illustration). In Fig.5 (f) we illustrate the results of Liu et al.’s [39] experiments with the K-means method and the three CVIs used here. As can be seen CH fails in identifying correctly the existing clusters when they are noisy, and S and DB fail when there are subclusters as indicated in Fig.5 (c). According to the results of Liu et al. [39] in the presence of noise or clusters with skewed distributions CH tends to predict more clusters than the truly existing ones. On the other hand, when there are subclusters, both S and BD tend to predict less clusters than the existing ones, due to the fact that they merge together small clusters. Then, the methods used here are somehow complimentary to each other and we should have in mind the situations where they clearly fail when analyzing the real-world datasets that will be studied in the next section.

**5.2. Real-world networks with ground truth.** Now we turn our attention to some real-world networks for which a sort of “ground-truth” for their partition into clusters exists. These networks constitute a benchmark for testing algorithms used for community detection in networks. Thus, we use them here to test the three CVIs

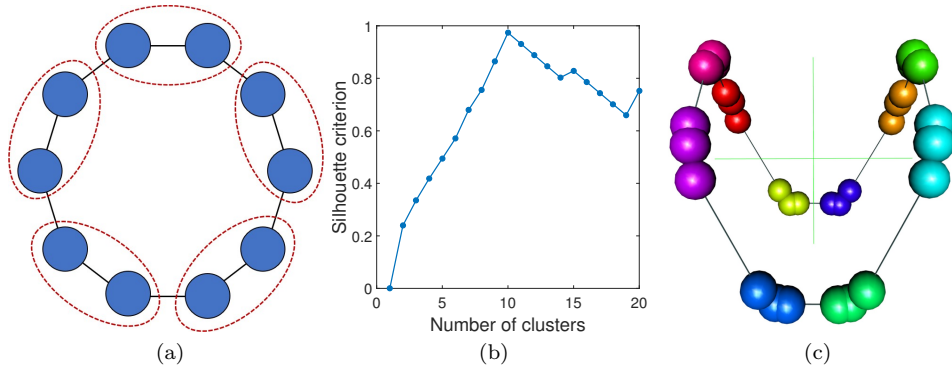


Fig. 4: (a) Illustration of a caveman graph in which modularity-based methods fail to detect the correct number of communities due to their merging of pairs of close clusters (clusters of nodes are represented as blue circles). (b) Plot of the variation of the Silhouette index for the different number of clusters in the graph illustrated in (a). Notice that the best performance is obtained for 10 clusters which is the correct number. (c) Illustration of the clusters obtained from the full-dimensional communicability angles and K-Means using Silhouette. The plot is obtained in the reduced 3D communicability space obtained from nonmetric multidimensional scaling.

used in the current work by using first the full-dimensional communicability angles matrices and the K-means method of clustering. In selecting the “best” approach we use the *Normalized Mutual Information* (NMI), as defined by Strehl and Ghosh [53] (see Supplementary Information), to measure the performance of the different algorithms on detecting clustering in comparison with the ground-truth. In addition to NMI we also report the *modularity index* for the partitions found as it is usually reported for network communities analysis [44]. We then apply our clustering algorithm to the following networks: the karate club of Zachary [58], the dolphin social network of Lusseau et al. [41], the network of political weblogs studied by Adamic and Glance [1] the network of books about politics studied by Krebs (see [44]), and the network of regular season games between Division I-A college football teams in the year 2000 [26]. The results obtained with the full-dimensional communicability angle matrices and K-means are given in Table 1. The results produced with the reduced 3D communicability angles space do not improve in any case those obtained with the full space and are not reported here. The main reason for that decision is that since information is lost in the dimensionality reduction process. it would be nonsense to apply the clustering algorithm to those if computational power allows to analyze the full communicability angles space data. We now compare these results with those reported in the literature using five different “popular” methods for community detection. These methods are: Louvain, FastGreedy, Infomap, Eigenvector and LP (for description of these methods and references see [19]). In Table 2 we give the values of the *NMI* and *Q* for the networks studied here. In addition we report the average value of *NMI* obtained for each network as well as the average of this parameter for every method. As can be seen Louvain, FastGreedy, Infomap and Eigenvector produce *NMI* in the range of 0.62-0.64 for all the five networks studied, and LP produces 0.71. Our method using of the three CVIs studied here produces superior

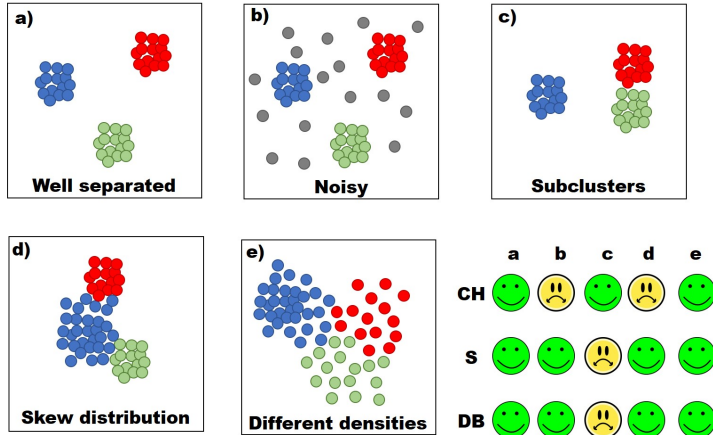


Fig. 5: Illustration of the impact of several cluster properties on the three CVIs used in this work according to Liu et al. The CVIs under consideration are *Calinski-Harabasz (CH) index*, *Silhouette (S) index* and *Davies-Bouldin (DB) index*. In the last panel a smiling face indicates that the method performs well on this situation and a sad face indicates that the method fails—under- or overestimate the number of clusters—on this situation.

network	ground truth		Silhouette			Calinski-Harabasz			Davies-Bouldin			Methods	
	C	Q	C	NMI	Q	C	NMI	Q	C	NMI	Q	NMI	Q
Karate	2	0.37	<b>2</b>	<b>1.00</b>	<b>0.37</b>	<b>2</b>	<b>1.00</b>	<b>0.37</b>	<b>2</b>	<b>1.00</b>	<b>0.37</b>	1.00	0.37
Dolphins	2	0.38	<b>2</b>	<b>0.89</b>	<b>0.38</b>	<b>2</b>	<b>0.89</b>	<b>0.38</b>	<b>2</b>	<b>0.89</b>	<b>0.38</b>	0.89	0.38
Football	12	0.55	11	0.91	0.66	12	0.91	0.64	13	0.90	0.66	0.91	0.66
PolBooks	2	0.41	<b>2</b>	<b>0.61</b>	<b>0.44</b>	7	0.58	0.45	<b>2</b>	<b>0.61</b>	<b>0.44</b>	0.60	0.44
PolBlogs	2	0.41	<b>2</b>	<b>0.72</b>	<b>0.52</b>	-	-	-	<b>2</b>	<b>0.72</b>	<b>0.52</b>	0.71	0.52
Average				0.83						0.82			

Table 1: Modularity  $Q$  and  $NMI$  for the 5 standard networks used for community detection using communicability angle and four different statistical clustering methods. C: number of clusters in the ground truth and detected for each community detection method. In bold cases where the number of clusters found by the methods coincide with the number of clusters present in the ground truth.

results for these 5 networks, with the exception of CH that fails to find clusters for the network of political blogs. For this network CH always predicts the highest possible number of clusters according to the range of values of  $K$  introduced in the K-means method. As we have seen before in the presence of noise or clusters with skewed distributions CH, tends to predict more clusters than the truly existing ones. In terms of the individual networks, our method produces the best results for the networks of karate club and dolphins using any of the three CVIs. For the network of football our method based on Silhouette produces similar results to the best performances obtained by Infomap and LP. For Political books and political blogs our results using Silhouette and Davies-Bouldin are far better than any of the five standard methods used for comparison. Thus, in general our method using either S or DB methods produces high standard clusters according to the metrics used here and for the set

network	Louvain		FastGreedy		Infomap		Eigenvector		LP		NMI
	NMI	Q	NMI	Q	NMI	Q	NMI	Q	NMI	Q	
Karate	0.59	0.42	0.69	0.38	0.70	0.40	0.68	0.39	0.70	0.40	0.73
Dolphins	0.48	0.52	0.61	0.50	0.50	0.52	0.54	0.49	0.69	0.50	0.64
Football	0.88	0.60	0.70	0.55	0.92	0.60	0.70	0.49	0.92	0.60	0.83
PolBooks	0.51	0.52	0.53	0.50	0.49	0.52	0.52	0.47	0.57	0.50	0.54
PolBlogs	0.63	0.43	0.65	0.43	0.48	0.42	0.69	0.42	0.69	0.43	0.64
Average	0.62		0.64		0.62		0.63		0.71		

Table 2: Modularity  $Q$  and  $NMI$  for the 5 standard networks used for community detection using 6 different methods from the literature. The average value of the  $NMI$  for each method is given as the last row of the Table. The average  $NMI$  obtained for each of the networks using the 6 methods considered is given as the last column of the Table.

of standard datasets considered. Finally, we illustrate the clusters obtained by the best CVI used before in K-Means for four of the five networks studied. In order to make these graphics we have projected the community structure onto the reduced 3D communicability space obtained by the nonmetric multidimensional scaling previously described. As can be seen there is a good separation of the clusters obtained that can be easily visualized in these reduced spaces.

### 5.3. Unsupervised clustering without ground truth.

**5.3.1. Analysis of a citation network.** Here we consider a citation network in which nodes represent papers that cite Milgram’s 1967 *Psychology Today* paper or use “*Small World*” in title, collected until July 23, 2002 [4]. Two nodes are connected if one of the papers cites the other. Although the network is directed we have symmetrized it for the current analysis. In this scenario we would like to investigate all the possible clusters existing in that network, which may represent group of papers coming from closely related scientific communities. Thus, our goal is to find the finest grain structure of such scientific communities in the network.

In this case Silhouette identifies 4 communicability clusters, Davies-Bouldin identifies 3 clusters and Calinski-Harabasz fails to identify any clustering as the index always increase with the maximum number of clusters to be identified. Both S and DB identifies a large cluster composed by 108 papers which mainly consists of papers published in Physics or multidisciplinary journals. DB includes 7 papers not included by S in this cluster, which are mainly from exogenous areas to the main subject in this cluster. They includes apart from a paper in the *European Physics Journal*, papers published in *Ethnology*, *American Sociological Review*, *IEEE Internet Computing*, *Society* and an *ACM* conference. The cluster identified by Silhouette is colored in cyan in Fig.7. The second cluster identified by DB is identical to the one identified by S and consists of 45 papers, which include Milgram’s itself (see red nodes in Fig. 7). This cluster mainly consists of papers in the area of quantitative social sciences and include papers about modifications of the “small-world” model, quantification of clustering, social distance, sociometric analysis, etc. It is not strange then that this cluster is the closest one to the cluster of physics papers. At this point, both S and DB diverges in the selection of the other clusters. Silhouette identifies two more clusters, one formed by 51 nodes (violet nodes in Fig.7) and another of 29 nodes (green nodes in Fig.7). However, DB identifies only one cluster that consists of the

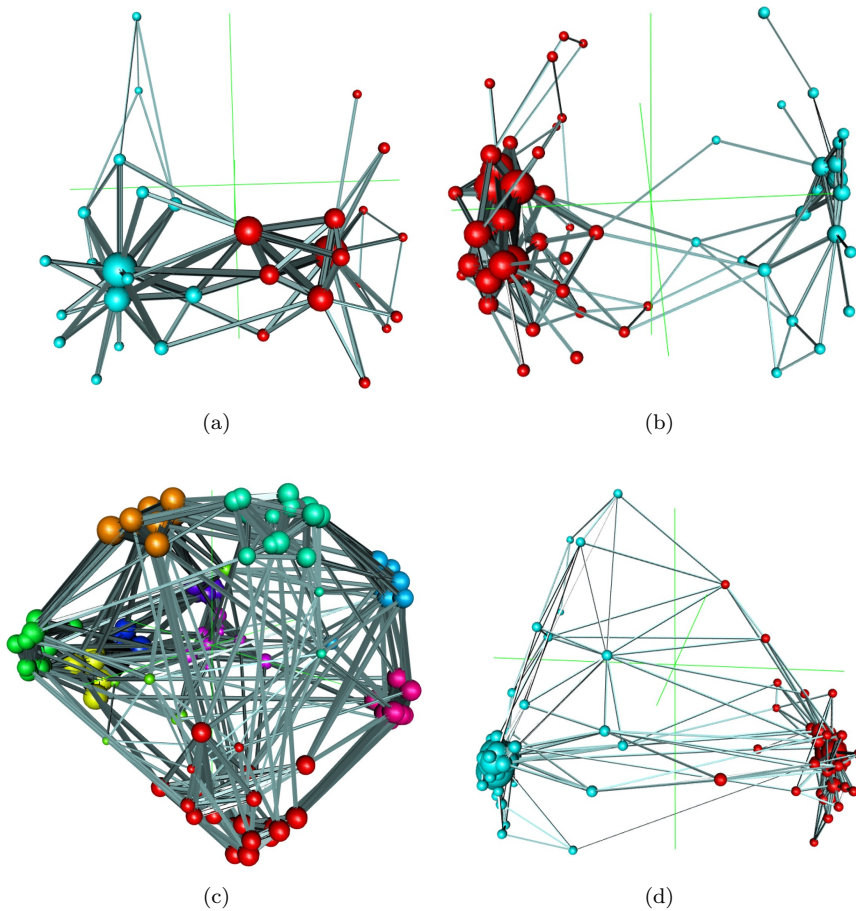


Fig. 6: Illustration of the clusters obtained by K-Means for the networks of karate club, dolphins, football and political books. The CVIs used for the detection of the best partition are described in the main text. The networks are embedded into the reduced 3D space obtained by nonmetric multidimensional scaling.

union of the two previously described clusters. It should be noticed that the difference in the Silhouette parameter for the partition into 3 and 4 clusters is marginal, i.e.,  $S = 0.8574$  for 4 clusters vs.  $S = 0.8569$  for 3 ones. However, as we want to know the finest-grain structure of this network we adopt here the division into 4 clusters. The cluster formed by 51 nodes is mainly formed by papers about organizational theory and the structure of social structures. The smallest cluster is mainly about papers on areas of applications, including medicine and epidemiology, psychology, information sciences, economics and education. Then, it is not rare that this cluster appears a little bit more isolated from the physics as well as from the mainstream sociology ones.

This example teaches us a fundamental difference between the density-based methods and the method presented here, which is based on communicability angles.

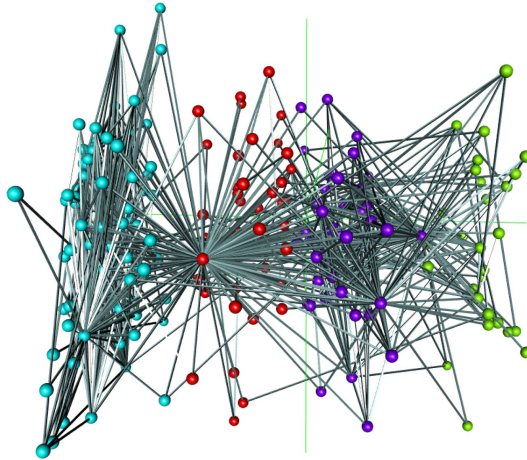


Fig. 7: Illustration of the 3D embedding of the citation network of “Small-World” in which papers that cite Milgram’s 1967 Psychology Today paper or use Small World in title, until July 23, 2002 are accounted. Two nodes are connected if one of the papers cites the other. Although the network is directed we have symmetrized it for the current analysis.

	$C_1$	$C_2$	$C_3$	$C_4$
$C_1$	0.992	4.601	7.596	12.491
$C_2$		1.066	3.019	7.919
$C_3$			0.968	4.930
$C_4$				1.208

Table 3: Average inter- and intra-cluster communicability angle for the clusters obtained using Silhouette method in the “Small-World” citation network.

For instance, the cluster 2 which is formed by 45 nodes has 50 edges inside the cluster. However, it has 78 edges connecting this cluster with cluster 3 and 63 edges connecting it with cluster 1. More critical is the case of cluster 4, the one having 29 nodes. It has 33 edges between nodes inside the cluster. However, it has 99 edges connecting this cluster with cluster 3. This makes that density-based methods split the network into a larger number of clusters. For instance, Infomap identifies 11 clusters in this network, from which 3 clusters are formed by only two nodes each and one cluster is formed by 3 nodes only. In contrast, the average communicability angle between pairs of nodes inside each of the 4 clusters identified here are significantly smaller than those between the nodes in different clusters (see Table 3).

**5.3.2. Analysis of a gene-gene network.** Now, we move to the analysis of a genetic network in which nodes represent genes that have been identified in relation to a human disease [27]. Two nodes are connected if the corresponding genes are involved in at least one common disease. In total there are 22 human diseases studied and a class of genes involved in mixed diseases, which was named in [27] as the “grey” class. In this case we have a previous information about certain “clusters”—not necessarily



topological in their nature—that exist in the network. We also know the finest grain structure of those clusters as we can know the specific disease in which every gene is involved in. For instance, one of the 22 disease categories consists of genes involved in cancer. Additionally, we could know which types of cancer compose that category creating a much larger number of categories or clusters for that network. Then, our goal here is not to study the finest-grain structure of that network but to find those clusters that group together some of these categories, possibly indicating interrelation between genes in several diseases. That is, we are interested here in finding a limited number of clusters in relation to the number of disease classes considered. In practical terms we will limit here the number of clusters to a maximum which is smaller than the number of groups existing, i.e., 22.

In this case Silhouette identifies 7 clusters and Davies-Bouldin identifies 8 ones (CH fails again by similar reasons as the ones described before). Some of the clusters identified by both CVIs are very similar to each other. Indeed, the Fowlkes–Mallows index [23] between the two clustering gives a value of 0.9772 which indicates 97% of similarity between the two clustering. Then, deciding which of the two clustering is the “best” is not a vital question here. In selecting one of the two clustering we are inclined to the one produced by the Davies-Bouldin Index, because it evaluates intra-cluster similarity and inter-cluster differences instead of the Silhouette Index which measures the distance between each data point, the centroid of the cluster to which it was assigned to and the closest centroid belonging to another cluster. We then proceed to the analysis of this clustering of the genes involved in human diseases. The first observation is that there are two clusters mainly related to cancer diseases, one (Fig.8 (a)) containing 37% of the genes in the cluster related to cancer and 29% of genes related to neurological diseases and the other (Fig.8 (e)) with 36% of genes involved in cancer, 21% in immunological diseases and 24% of mixed involvement. Cluster 2 (Fig.8 (b)) has almost equal contributions from genes involved in Cardiovascular, Dermatological and Ear/Nose/Throat diseases and 31% of genes with mixed involvement. Cluster3 (Fig.8 (c)) is mainly formed by genes involved in ophthalmological diseases and cluster 4 (Fig.8 (d)) is mainly populated by genes related to hematological disorders. Clusters 6-8 have participation of genes involved in cardiovascular, neurological and psychiatric diseases, nutritional and endocrine disorders as well as neurological and immunological ones.

We are not going to make an exhaustive analysis of each of the clusters previously found but we will conduct a couple of experiments in order to indirectly validate the biological significance of the clusters found. The dataset used for the creation of the gene-gene network compiled here used information about the involvement of genes in human diseases as reported until 2007, in which the paper of Goh et al. [27] was published. Then, we selected two of the clusters found here for our further analysis. The first is cluster 1 which is formed by 239 genes, two thirds of which are involved either in cancer or in neurological diseases. According to the criterion used by Goh et al. [27] in building their network, a gene classified in the disease class “neurological” is not involved (as reported until 2007) in any other non-neurological disorder. Otherwise, it is grouped as “grey”. This means that a gene grouped in the class of “neurological diseases was not known in 2007 to be involved also in “cancer”. However, our clustering method groups together 88 genes involved in cancer with 69 genes involved in neurological disorders in the same cluster. Consequently, we formulate the hypothesis that:

**Hypothesis 1.** Genes involved in neurological disorders which are in cluster 1 can also be involved in cancer due to certain similarity in their topological environment

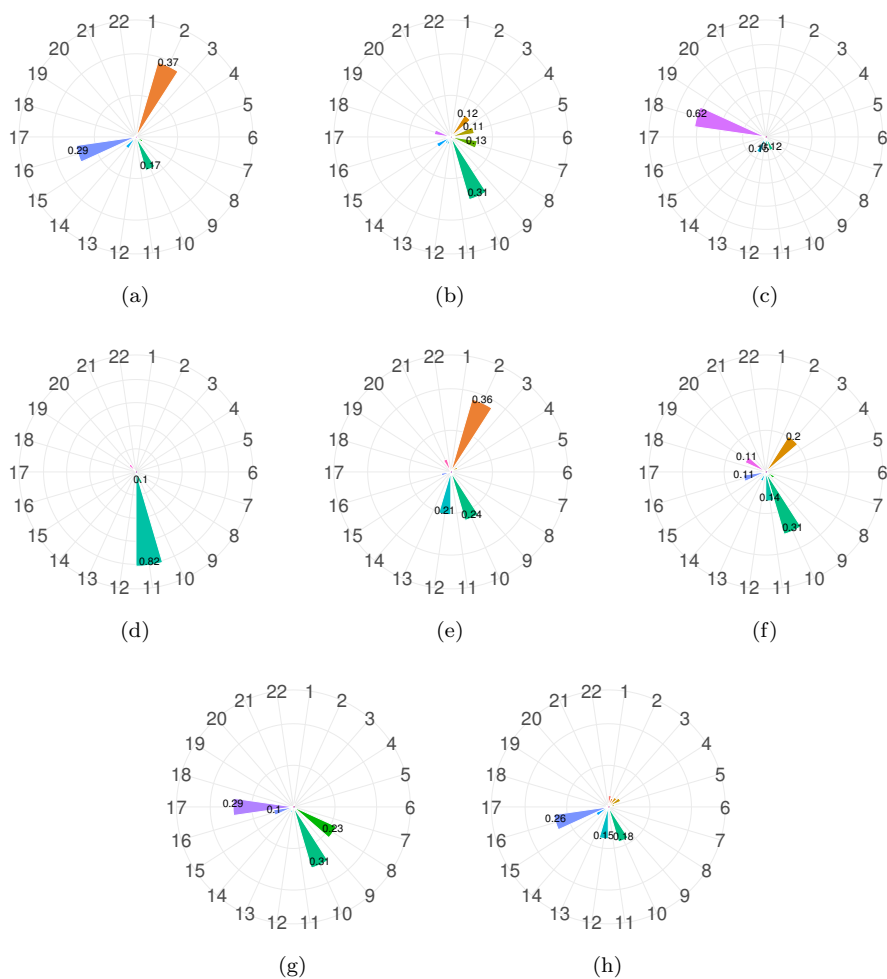


Fig. 8: Radial histogram of the contribution of each of the 22 human diseases considered to the clusters of genes obtained in this work. The diseases are represented by a number according to the following code: 1: Bone; 2: Cancer; 3: Cardiovascular; 4: Connective tissue; 5: Dermatological; 6: Developmental; 7: Ear/Nose/Throat; 8: Endocrine; 9: Gastrointestinal; 10: Mixed; 11: Hematological; 12: Immunological; 13: Metabolic; 14: Multiple; 15: Muscular; 16: Neurological; 17: Nutritional; 18: Ophthalmological; 19: Psychiatric; 20: Renal; 21: Respiratory; 22: Skeletal.

in the gene-gene network.

In order to test this hypothesis we carried out a bibliographic search for all the genes in cluster 1 which were involved in neurological disorders to find whether they have been recently reported in cancer. Our search is based on the scientific literature published since 2006, a year before the year in which Goh et al. [27] paper was published. In Table 4 we report 19 genes that are known to be related to neurological diseases such as ataxia, Amyotrophic Lateral Sclerosis (ALS), Parkinson, epilepsy and Charcot-Marie-Tooth disease, which are in cluster 1. In addition, in the most

recent literature we have found evidences of the involvement of these genes in breast, colorectal, ovarian, lung, prostate, and other types of cancer. Although our search has not being exhaustive, the current findings point out to the fact that the clusters found in this work may contain important biological information. In particular, that genes clustered in the same group but having involvement in different diseases may have some “promiscuity” in the sense of being responsible for several diseases, such as the ones reported in Table 4 for neurological diseases and cancer (all the references for the new findings are reported in a Supplementary Information accompanying this paper). We should point out that there are other 50 genes in this cluster which were reported as involved in neurological diseases and for which we did not find any connection with cancer. These genes could be target of experimental search for involvement in different types of cancer also confirming our hypothesis 1.

No.	gene	neurological	cancer
1	NDRG1	Charcot-Marie-Tooth	breast
2	FGF14	Spinocerebellar ataxia	breast
3	NEFH	ALS	breast
4	PPP2R2B	Spinocerebellar ataxia	breast
5	SLC25A22	epilepsy	breast, colorectal,
6	GABRA1	epilepsy	colorectal
7	JPH3	Huntington’s	colorectal
8	GJB1	Charcot-Marie-Tooth	colorectal
9	UCHL1	Parkinson	colorectal, ovarian
10	DNM2	Charcot-Marie-Tooth	ovarian
11	TDP1	Spinocerebellar ataxia	lung
12	SOD1	ALS	lung
13	PARK7	Parkinson	lung, prostate
14	LRRK2	Parkinson	non-skin
15	KIF1B	Charcot-Marie-Tooth	hepatocellular carcinoma
16	HSPD1	Spastic ataxia/paraplegia	colon
17	NR4A2	Parkinson	gastrointestinal
18	Rab7	Charcot-Marie-Tooth	thyroid adenoma
19	SNCAIP	Parkinson	medulloblastome

Table 4: List of genes which were grouped in cluster 1 due to their involvement in neurological diseases and which have been recently reported to be involve in cancer as correspond to 37% of genes in cluster 1.

The second example is related to cluster 5, which is formed by 107 genes from which 1/3 of genes are involved in cancer and a quarter of genes were classified in the group “grey”. The group grey was created by Goh et al. [27] for grouping all those genes which were involved in more than one type of human disease group. That is, if a gene is involved in two different kinds of neurological diseases, e.g. ataxia and paraplegia, it is still considered as in the class of neurological diseases. However, a gene like APOA1, which is involved in Alzheimer disease (neurological), Hyperlipoproteinemia (metabolic), and Myocardial infarction (cardiovascular), is considered in the class “grey”. In cluster 5 there are 26 genes in class “grey”. From these 26 genes, 12 genes were already reported to be involved in cancer by Goh et al. [27] when they grouped them in the class “grey”. Then, there are 14 genes in this cluster which are involved in different diseases but that were not reported to be involved in cancer by Goh et al. [27]. Consequently, we elaborate our second hypothesis.

**Hypothesis 2.** Genes involved in multiple diseases which are in cluster 5 can also be involved in cancer due to certain similarity in their topological environment

in the gene-gene network.

In Table 5 we report our findings for 10 out of the 14 remaining “grey” genes in cluster 5, which have been recently reported to be involved in several types of cancer. All the references for the new reports are given in a Supplementary Information accompanying this paper. Here again these results indirectly validate the biological significance of the clusters found in this work using unsupervised learning based on networks embedded into hyperspheres.

No.	gene	“grey” diseases	cancer
1	ABCA1	Cerebral amyloid angiopathy, Coronary artery disease, HDL cholesterol level QTL, Tangier disease	prostate cancer
2	ESR1	Estrogen-resistance, HDL cholesterol level QTL, Migraine	hormone-resistant metastatic breast cancer
3	ALOX5	Asthma, Atherosclerosis	chronic myeloid leukemia
4	IL10	Graft -versus-host disease, HIV, Rheumatoid arthritis	prostate cancer
5	IL13	Allergic rhinitis, Asthma	colon cancer
6	CIITA	Bare lymphocyte syndrome, Multiple sclerosis, Rheumatoid arthritis	lymphoid cancers
7	PTPRC	Multiple sclerosis, Severe combined immunodeficiency	lymphoblastic leukemia
8	BDNF	Central hypoventilation syndrome, Memory impairment, Obsessive-compulsive disorder	lung cancer
9	PLA2G7	Asthma, Atopy, Platelet defect/deficiency	prostate cancer
10	CD36	Malaria, Platelet defect/deficiency	glioblastoma

Table 5: List of genes grouped in cluster 5 which were reported as being involved in several diseases (“grey” diseases) but not in cancer until 2007. All these genes have been recently found as being involved in different types of cancer in correspondence with the majority of genes in this cluster.

**6. Conclusions.** In this work we propose a way to extract network information by considering machine learning techniques applied over a Euclidean hyperdimensional representation of relational data. It should be remarked that this “geometric learning” approach differs from others in the literature in the following. While many geometric learning methods are based on imposed embeddings of the network in given spaces, here we exploit a natural embedding of the graph emerging from the flow of items through its nodes and edges. This space is a Euclidean  $(n - 1)$ -sphere, where  $n$  is the number of nodes of the graph. Here we have used geometric unsupervised learning approaches to find clusters in networks. In these clusters the nodes are grouped not by their intra- and inter-cluster densities, but on the basis of their capacity of successfully delivering items through the network. We also used nonmetric multidimensional scaling to reduce the dimensionality of the hyperspheres in which the networks are naturally embedded to 3-dimensional ones that allow visualization of the systems represented. It is important to remark that the value of the current work is not in the sophistication of the machine learning techniques used but in the novelty of this representation systems of networks. Thus, further development using more advanced machine learning and deep learning techniques will surely open new possibilities for extracting high-quality structural information from relational data, such as complex networks.

- [1] L. A. ADAMIC AND N. GLANCE, *The political blogosphere and the 2004 U.S. election: divided they blog*, 2005.
- [2] F. AZUAJE, *Witten IH, Frank E: Data Mining: Practical machine learning tools and techniques 2nd edition*, BioMedical Engineering OnLine, 5 (2006), p. 51.
- [3] A.-L. BARABÁSI AND R. ALBERT, *Emergence of scaling in random networks*, Science, 286 (1999), pp. 509–512.
- [4] V. BATAGELJ AND A. MRVAR, *Pajek datasets*, 2006.
- [5] S. BOCCALETTI, V. LATORA, Y. MORENO, M. CHAVEZ, AND D. U. HWANG, *Complex networks: Structure and dynamics*, Physics Reports, 424 (2006), pp. 175–308.
- [6] I. BORR AND P. GROENEN, *Modern Multidimensional Scaling: Theory and Applications*, Springer New York, 2013.
- [7] M. M. BRONSTEIN, J. BRUNA, Y. LECUN, A. SZLAM, AND P. VANDERGHEYNST, *Geometric deep learning: Going beyond Euclidean data*, IEEE Signal Processing Magazine, 34 (2017), pp. 18–42.
- [8] T. CALISKI AND J. HARABASZ, *A dendrite method for cluster analysis*, Communications in Statistics, 3 (1974), pp. 1–27.
- [9] D. L. DAVIES AND D. W. BOULDIN, *A cluster separation measure*, IEEE Transactions on Pattern Analysis and Machine Intelligence, PAMI-1 (1979), pp. 224–227.
- [10] P. DOMINGOS, *A few useful things to know about machine learning*, Commun. ACM, 55 (2012), pp. 78–87.
- [11] X. DONG, P. FROSSARD, P. VANDERGHEYNST, AND N. NEFEDOV, *Clustering on multi-layer graphs via subspace analysis on grassmann manifolds*, IEEE Transactions on Signal Processing, 62 (2014), pp. 905–918.
- [12] E. ESTRADA, *The Structure of Complex Networks: Theory and Applications*, Oxford University Press, Inc., 2011.
- [13] E. ESTRADA AND N. HATANO, *Communicability in complex networks*, Physical Review E, 77 (2008), p. 036111.
- [14] E. ESTRADA AND N. HATANO, *Communicability angle and the spatial efficiency of networks*, SIAM Review, 58 (2016), pp. 692–715.
- [15] E. ESTRADA, N. HATANO, AND M. BENZI, *The physics of communicability in complex networks*, Physics Reports, 514 (2012), pp. 89–119.
- [16] E. ESTRADA AND D. J. HIGHAM, *Network properties revealed through matrix functions*, SIAM Review, 52 (2010), pp. 696–714.
- [17] E. ESTRADA AND J. A. RODRÍGUEZ-VELÁZQUEZ, *Subgraph centrality in complex networks*, Physical Review E, 71 (2005), p. 056103.
- [18] E. ESTRADA, M. G. SÁNCHEZ-LIROLA, AND J. A. D. L. PEÑA, *Hyperspherical embedding of graphs and networks in communicability spaces*, Discrete Appl. Math., 176 (2014), pp. 53–77.
- [19] S. FORTUNATO, *Community detection in graphs*, Physics Reports, 486 (2010), pp. 75–174.
- [20] S. FORTUNATO AND M. BARTHÉLEMY, *Resolution limit in community detection*, Proceedings of the National Academy of Sciences, 104 (2007), pp. 36–41.
- [21] S. FORTUNATO AND C. CASTELLANO, *Community structure in graphs*, in Computational Complexity: Theory, Techniques, and Applications, R. A. Meyers, ed., Springer New York, New York, NY, 2012, pp. 490–512.
- [22] S. FORTUNATO AND D. HRIC, *Community detection in networks: A user guide*, Physics Reports, 659 (2016), pp. 1–44.
- [23] E. B. FOWLKES AND C. L. MALLOWS, *A method for comparing two hierarchical clusterings*, Journal of the American Statistical Association, 78 (1983), pp. 553–569, <https://doi.org/10.1080/01621459.1983.10478008>, <https://www.tandfonline.com/doi/abs/10.1080/01621459.1983.10478008>.
- [24] K. R. GABRIEL AND R. R. SOKAL, *A new statistical approach to geographic variation analysis*, Systematic Biology, 18 (1969), pp. 259–278.
- [25] G. GAN, C. MA, AND J. WU, *Data Clustering: Theory, Algorithms, and Applications*, Data Clustering: Theory, Algorithms, and Applications.
- [26] M. GIRVAN AND M. E. J. NEWMAN, *Community structure in social and biological networks*, Proceedings of the National Academy of Sciences, 99 (2002), pp. 7821–7826.
- [27] K.-I. GOH, M. E. CUSICK, D. VALLE, B. CHILDS, M. VIDAL, AND A.-L. BARABSI, *The human disease network*, Proceedings of the National Academy of Sciences, 104 (2007), pp. 8685–8690.
- [28] M. HALKIDI, Y. BATISTAKIS, AND M. VAZIRGIANNIS, *On clustering validation techniques*, Journal of Intelligent Information Systems, 17 (2001), pp. 107–145.
- [29] A. K. JAIN, *Data clustering: 50 years beyond k-means*, Pattern Recognition Letters, 31 (2010),

- pp. 651–666.
- [30] A. K. JAIN AND R. C. DUBES, *Algorithms for clustering data*, Prentice-Hall, Inc., 1988.
  - [31] J. W. JAROMCZYK AND G. T. TOUSSAINT, *Relative neighborhood graphs and their relatives*, Proceedings of the IEEE, 80 (1992), pp. 1502–1517.
  - [32] M. I. JORDAN AND T. M. MITCHELL, *Machine learning: Trends, perspectives, and prospects*, Science, 349 (2015), pp. 255–260.
  - [33] G. KARYPIS, H. EUI-HONG, AND V. KUMAR, *Chameleon: hierarchical clustering using dynamic modeling*, Computer, 32 (1999), pp. 68–75.
  - [34] L. KAUFMAN AND P. J. ROUSSEEUW, *Finding Groups in Data: An Introduction to Cluster Analysis*, Wiley Series in Probability and Statistics, John Wiley & Sons, 2005.
  - [35] J. B. KRUSKAL, *Multidimensional scaling by optimizing goodness of fit to a nonmetric hypothesis*, Psychometrika, 29 (1964), pp. 1–27.
  - [36] J. B. KRUSKAL, *Nonmetric multidimensional scaling: A numerical method*, Psychometrika, 29 (1964), pp. 115–129.
  - [37] V. LATORA, V. NICOSIA, AND G. RUSSO, *Complex Networks: Principles, Methods and Applications*, Cambridge University Press, 2017.
  - [38] H. LIU, S. SHAH, AND W. JIANG, *On-line outlier detection and data cleaning*, Computers & Chemical Engineering, 28 (2004), pp. 1635–1647.
  - [39] Y. LIU, Z. LI, H. XIONG, X. GAO, AND J. WU, *Understanding of internal clustering validation measures*, 2010.
  - [40] C.-T. LU, D. CHEN, AND Y. KOU, *Algorithms for spatial outlier detection*, 2003.
  - [41] D. LUSSEAU, K. SCHNEIDER, O. J. BOISSEAU, P. HAASE, E. SLOOTEN, AND S. M. DAWSON, *The bottlenose dolphin community of Doubtful Sound features a large proportion of long-lasting associations*, Behavioral Ecology and Sociobiology, 54 (2003), pp. 396–405.
  - [42] L. MA, X. JIANG, K. WU, Z. ZHANG, S. TANG, AND Z. ZHENG, *Surveying network community structure in the hidden metric space*, Physica A: Statistical Mechanics and its Applications, 391 (2012), pp. 371–378.
  - [43] M. E. J. NEWMAN, *The structure and function of complex networks*, SIAM Review, 45 (2003), pp. 167–256.
  - [44] M. E. J. NEWMAN, *Modularity and community structure in networks*, Proceedings of the National Academy of Sciences, 103 (2006), pp. 8577–8582.
  - [45] A. Y. NG, M. I. JORDAN, AND Y. WEISS, *On spectral clustering: analysis and an algorithm*, 2001.
  - [46] E. PAUL AND R. ALFRD, *On random graphs I*, Publicationes Mathematicae (Debrecen), 6 (1959).
  - [47] G. PIATETSKY-SHAPIRO, *Discovery, analysis and presentation of strong rules*, in Knowledge Discovery in Databases, G. Piatetsky-Shapiro and W. J. Frawley, eds., AAAI Press, 1991, pp. 229–248.
  - [48] M. A. PORTER, J. P. ONNELA, AND P. J. MUCHA, *Communities in networks*, Notices of the American Mathematical Society, 56 (2009), pp. 1082–1097.
  - [49] P. J. ROUSSEEUW, *Silhouettes: A graphical aid to the interpretation and validation of cluster analysis*, Journal of Computational and Applied Mathematics, 20 (1987), pp. 53–65.
  - [50] S. E. SCHAEFFER, *Graph clustering*, Computer Science Review, 1 (2007), pp. 27–64.
  - [51] T. SILVA AND L. ZHAO, *Machine Learning Complex Networks*, Springer International Publishing, 1 ed., 2016.
  - [52] D. STEINLEY, *Kmeans clustering: A half century synthesis*, British Journal of Mathematical and Statistical Psychology, 59 (2006), pp. 1–34.
  - [53] A. STREHL AND J. GHOSH, *Cluster ensembles — a knowledge reuse framework for combining multiple partitions*, J. Mach. Learn. Res., 3 (2003), pp. 583–617.
  - [54] G. T. TOUSSAINT, *The relative neighbourhood graph of a finite planar set*, Pattern Recognition, 12 (1980), pp. 261–268.
  - [55] L. VAN DER MAATEN, E. POSTMA, AND H. HERIK, *Dimensionality Reduction: A Comparative Review*, vol. 10, 2007.
  - [56] U. VON LUXBURG, *A tutorial on spectral clustering*, Statistics and Computing, 17 (2007), pp. 395–416.
  - [57] B. XIAO AND E. R. HANCOCK, *Geometric characterisation of graphs*, Image Analysis and Processing ICIAP 2005, Berlin, Heidelberg, 2005, Springer Berlin Heidelberg, pp. 471–478.
  - [58] W. ZACHARY, *An information flow model for conflict and fission in small groups*, Journal of Anthropological Research, 33 (1977), pp. 452–473.
  - [59] L. ZHOU, S. PAN, J. WANG, AND A. V. VASILAKOS, *Machine learning on big data*, Neurocomput., 237 (2017), pp. 350–361.